Post-exposure protection of SARS-CoV-2 lethal infected K18-hACE2 transgenic mice by neutralizing human monoclonal antibody

Ronit Rosenfeld*, Tal Noy-Porat, Adva Mechaly, Efi Makdasi, Yinon Levy, Ron Alcalay, Reut Falach, Moshe Aftalion, Eyal Epstein, David Gur, Theodor Chitlaru, Einat B. Vitner, Sharon Melamed, Boaz Politi, Ayelet Zauberman, Shirley Lazar, Adi Beth-Din, Yentl Evgy, Shmuel Yitzhaki, Shmuel C. Shapira, Tomer Israely and Ohad Mazor*

Israel Institute for Biological Research, Ness-Ziona, Israel

*Address correspondence to:
Ronit Rosenfeld; Ohad Mazor
Israel Institute for Biological Research
Ness-Ziona 74100, Israel
E-mail: ronitr@iibr.gov.il; ohadm@iibr.gov.il

Abstract

Coronavirus disease 2019 (COVID-19) pandemic, caused by the severe acute respiratory syndrome coronavirus 2 (SARS-CoV-2), exhibits high levels of mortality and morbidity and has dramatic consequences on human life, sociality and global economy. Neutralizing antibodies constitute a highly promising approach for treating and preventing infection by this novel pathogen. In the present study, we characterized and further evaluated the recently identified human monoclonal MD65 antibody for its ability to provide protection against a lethal SARS-CoV-2 infection of K18-hACE2 transgenic mice. Eighty percent of the untreated mice succumbed 6-9 days post-infection while administration of the MD65 antibody as late as 3 days after exposure, rescued all infected animals. In addition, the efficiency of the treatment is supported by prevention of morbidity and ablation of the load of infective virions in the lungs of treated animals. The data unprecedentedly demonstrate, the therapeutic value of human monoclonal antibodies as a life-saving treatment of severe COVID-19 infection.

Introduction

Human monoclonal antibodies (mAbs), specifically targeting surface viral proteins, have increasingly demonstrated prophylactic and therapeutic efficacy against various viruses including HIV, Ebola, and the pathogenic beta-coronaviruses MERS-CoV and SARS-CoV[1-5]. Neutralizing antibodies constitute a highly promising approach for treating and preventing infection by the novel SARS-CoV-2[6]. The viral surface spike glycoprotein, is essential for viral attachment, fusion and entry into human cells and thus considered as the major target for therapeutic neutralizing antibodies[7-13]. Specifically, highly potent neutralizing antibodies target and block the binding of the receptor binding domain (RBD) located in the S1 subunit of the spike, to the human angiotensin-converting enzyme 2 (hACE2)[7,10,14].

A reliable animal model for COVID-19, is essential for the development of anti-SARS-CoV-2 countermeasures and for deciphering the pathogenicity of the disease[15]. Accordingly, mouse models that exploit the recombinant hACE2 expression, either by transgenic or viral-transduction approaches were developed[16-28]. A transgenic mouse strain expressing hACE2 under the K18 promoter (K18-hACE2) was shown to be highly susceptible to SARS-CoV-2 infection, resulting in significant viral load in the lungs, heart, brain and spleen as well as mortality[26,27,29]. In response to the urgent need for antibody-based therapy for COVID-19, several reports have demonstrated efficacy against SARS-CoV-2 infection by neutralizing antibodies, primarily as prophylactic protection[10,19,30-32]. These studies were based on non-lethal COVID-19 models of mice transduced to express hACE2, and did not demonstrate the efficacy of Ab-based passive therapy administered at a significant time post-infection.

We have previously reported the isolation of human neutralizing Abs selected against SARS-CoV-2 RBD by extensive screening of a phage-display library generated from lymphocytes collected from infected individuals. Among these Abs, MD65 exhibited the highest neutralization potency *in vitro*[11]. The aim of the current study was to evaluate the therapeutic efficacy of this Ab in a lethal COVID-19 animal model by assessing its prophylaxis and treatment abilities to protect K18-hACE2 infected mice.

Methods

Recombinant proteins expression

Mammalian cell codon optimized nucleic sequence, coding for the SARS-CoV-2 Spike glycoprotein [GenPept: QHD43416 ORF (https://www.ncbi.nlm.nih.gov/protein/1791269090)], was used to design pcDNA3.1^{+} based expression plasmids, mediating recombinant expression of the soluble spike (amino acids 1-1207), S1 (amino acids 1-685) and RBD (amino acids 1–15 and 318–542) proteins. Same expression vector utilized for cloning and production of the secreted form of the human angiotensin-converting enzyme 2 (hACE2) receptor [amino acids 1-740; GenPept: NP_068576.1 ORF (https://www.ncbi.nlm.nih.gov/protein/ NP_068576.1)]. C-terminal his-tag as well as a strep-tag, were included in order to facilitate protein purification. Expression of the recombinant proteins was performed using ExpiCHO™ Expression system (Thermoscientific, USA, Cat# A29133) following purification using HisTrap™ (GE Healthcare, UK) and Strep-Tactin®XT (IBA, Germany).

MD65 scFv, derived from a phage-display library, was initially cloned as a scFv-Fc Ab, as recently described[11]. To generate a full-length IgG, the VH and VL fragments where re-cloned into pcDNA3.1-Heavy and pcDNA3.1-Kappa vectors, respectively. These vectors, were designed to include IgG1 and Kappa chain constant domains, as well as the appropriate signal sequences for the production of complete heavy and light chains. The resulting antibody was further engineered to include three point mutations in its Fc region: M252Y/S254T/T256E (YTE mutations). These mutations were previously shown to increase antibody affinity to the human FcRn, at pH 6.0 and hence, to improve the Ab's serum half-life in rhesus macaques and humans[33,35,36]. The antibody MD29 scFc-Fc, reported to target RBD and neutralize SARS-CoV-2 but not inhibit ACE2-RBD interaction[11], was similarly cloned and expressed as IgG-YTE.

Recombinant antibodies (scFv-Fc, IgG and IgG-YTE) were expressed using ExpiCHO™ Expression system (Thermoscientific, USA, Cat# A29133) and purified on HiTrap Protein-A column (GE healthcare, UK).

All purified proteins were sterile-filtered and stored in PBS. The integrity and purity of the recombinant expressed proteins were confirmed by SDS-PAGE analysis (Supplementary Fig. 4).

ELISA

Direct ELISA was performed against SARS-CoV-2 S1 subunit (expressed and purified as recently described[11]) for binding evaluation and for Ab concentration determination. Maxisorp 96-well microtiter plates (Nunc, Roskilde, Denmark) were coated overnight with 1 μg/ml of S1 protein in NaHCO3 buffer (50 mM, pH 9.6), washed, and blocked with PBST at room temperature for 1 h. Human Abs were visualized by AP-conjugated Donkey anti-human IgG (Jackson ImmunoResearch, USA, Cat# 709-055-149, lot 130049) used at 1:1,000 and further developed with PNPP substrate (Sigma, Israel, Cat# N1891). For the quantification of MD65 Ab presence in plasma or sera samples, standard curve included purified MD65 IgG-YTE Ab at the concentration range of 2-3000 ng/ml (diluted in PBST). Correct ELISA-based quantification was confirmed by 4 non-immune sera samples (collected prior to Ab-administration) containing exogenously-added known concentration of the Ab. Standard curves confirmed as above, were calculated for each individual ELISA plate/data set.

The endogenous humoral response was tested in mice sera samples collected at 14 dpi, evaluated by ELISA against SARS-CoV-2 spike, S1 and RBD essentially as described above, using AP-conjugated Donkey anti-mouse IgG (H+L) minimal cross (Jackson ImmunoResearch, USA, Cat# 715-055-150, lot 142717) used at 1:2,000.

Biolayer interferometry (BLI) analysis

Binding studies were carried out using the Octet system (ForteBio, USA, Version 8.1, 2015) which measures biolayer interferometry (BLI). All steps were performed at 30°C with shaking at 1,500 rpm in a black 96-well plate containing 200 μl solution in each well. For hACE2 competitive binding assay, streptavidin-coated biosensors were loaded with biotinylated MD65 (10 μg/ml), as either scFv-Fc, IgG or IgG-YTE antibody formats. Antibody-loaded sensors were first incubated with RBD (12 μg/ml), washed and incubated with hACE2 (20 μg/ml). MD29 Ab, previously shown to bind RBD without blocking its binding to hACE2[11], was used as a control.

For the evaluation of MD65 affinity to human FcRn, anti-Fab coated sensors were loaded with MD65 IgG or IgG-YTE (30 μg/ml), to reach 2.5 nm wavelength shift, and then washed. Sensors were then incubated with different concentrations of FcRn (Sino Biological #CT009-H08H; ranging from 75 to 300 nM) in pH 6.0, for 60 sec (association phase) and transferred to buffer-containing wells for additional 60 sec

(dissociation phase). Binding and dissociation were measured as changes over time in light interference after subtraction of parallel measurements from unloaded biosensors. Sensorgrams were fitted with a 1:1 binding model using the Octet data analysis software 8.1 (Fortebio, USA, 2015). All BLI experiments were repeated several times.

Cells

Vero E6 (ATCC® CRL-1586™) were obtained from the American Type Culture Collection. Cells were grown in Dulbecco's modified Eagle's medium (DMEM) supplemented with 10% fetal bovine serum (FBS), MEM non-essential amino acids (NEAA), 2 mM L-Glutamine, 100 Units/ml Penicillin, 0.1 mg/ml Streptomycin and 12.5 Units/ml Nystatin (P/S/N) (Biological Industries, Israel). Cells were cultured at 37°C, 5% CO_2 at 95% air atmosphere.

ExpiCHO-S (Thermoscientific, USA, Cat# A29127) were used for expression of recombinant proteins as described above.

Plaque reduction neutralization test (PRNT)

Handling of SARS-CoV-2 was conducted in a BSL3 facility in accordance with the biosafety guidelines of the Israel Institute for Biological Research (IIBR). SARS-CoV-2 (GISAID accession EPI_ISL_406862) strain was kindly provided by Bundeswehr Institute of Microbiology, Munich, Germany. Virus stocks were propagated and tittered by infection of Vero E6 cells as recently described[44]. For plaque reduction neutralization test (PRNT), Vero E6 cells were plated overnight (as detailed above) at a density of 5×10^5 cells/well in 12-well plates. Antibody samples were 2-fold serially diluted (ranging from 2 to 0.015 μg/ml) in 400 μl of MEM supplemented with 2% FBS, NEAA, 2 mM L-Glutamine and P/S/N. 400 μl containing 500 PFU/ml of SARS-CoV-2 virus were then added to the Ab solution supplemented with 0.25% guinea pig complement sera (Sigma, Israel) and the mixture incubated at 37°C, 5% CO_2 for 1 h. Monolayers were then washed once with DMEM w/o FBS and 200 μl of each Ab-virus mixture was added in triplicates to the cells for 1 h. Virus mixture w/o Ab was used as control. 2 ml/well overlay [MEM containing 2% FBS and 0.4% Tragacanth (Sigma, Israel)] were added to each well and plates were further incubated at 37°C, 5% CO2 for 48 h. Following incubation, the overlay was aspirated and the cells were fixed and stained with 1 ml of crystal

violet solution (Biological industries, Israel). The number of plaques in each well was scored and the NT_{50} (Ab concentration at which the plaque number was reduced by 50%, compared to plaque number of the control, in the absence of Ab), was calculated using the Prism software version 8 (GraphPad Software Inc., USA).

Animal experiments

Treatment of animals was in accordance with regulations outlined in the U.S. Department of Agriculture (USDA) Animal Welfare Act and the conditions specified in the Guide for Care and Use of Laboratory Animals (National Institute of Health, 2011). Animal studies were approved by the local ethical committee on animal experiments (protocol number M-51-20 and M-56-20). Male and female K18-hACE2 transgenic (B6.Cg-Tg(K18-ACE2)2Prlmn/J HEMI) and C57BL/6 mice (Jackson Laboratories, USA) were maintained at 20−22 °C and a relative humidity of 50 ± 10% on a 12 h light/dark cycle, fed with commercial rodent chow (Koffolk Inc.) and provided with tap water *ad libitum*. All animal experiments involving SARS-CoV-2 were conducted in a BSL3 facility.

Infection experiments were carried out using SARS-CoV-2, isolate Human 2019-nCoV ex China strain BavPat1/2020 that was kindly provided by Prof. Dr. Christian Drosten (Charité, Berlin, Germany) through the European Virus Archive – Global (EVAg Ref-SKU: 026V-03883). The original viral isolate was amplified by 5 passages and quantified by plaque titration assay in Vero E6 cells, and stored at -80°C until use. The viral stock DNA sequence and coding capacity were confirmed as recently reported[45].

SARS-CoV-2 BavPat1/2020 virus diluted in PBS supplemented with 2% FBS (Biological Industries, Israel) was used to infect animals by intranasal instillation of anesthetized mice. For Abs protection evaluation, mice were treated with two doses (4 days apart) of 1 mg/mouse of MD65 Ab, first administered IP either 4 h prior, or 1-4 days post-infection with 200 PFU of SARS-CoV-2. Dose-dependency experiments were performed by single administration of 1, 0.1 and 0.01 mg/mouse (equivalent of 50, 5, and 0.5 mg/Kg body weight, respectively) of the MD65 antibody 2 days following infection with 300 PFU SARS-CoV-2. Control groups were administered with PBS or isotype control Ab (anti ricin MH75 Ab) at the indicated times. Body weight was monitored daily throughout the follow-up period post infection. Mice

were evaluated once a day for clinical signs of disease and dehydration. Euthanasia was applied when the animals exhibited irreversible veterinary-evaluated disease symptoms (rigidity, lack of any visible reaction to contact).

Pharmacokinetics

Pharmacokinetics was determined in male and female C57BL/6 mice following administration of 0.2 mg MD65 IgG-YTE Ab either by intravenous (IV; n=4; 200 µl of 1 mg/ml Ab) or intraperitoneal [IP; n=5; 1 ml of 0.2 mg/ml Ab] route. At different time points, 5 µl blood samples were drawn from the tail vein, diluted 20-fold in PBS, and centrifuged for 10 min at 500 g for the removal of red blood cells. Supernatant plasma fractions were stored at -20°C until tested in ELISA for the Ab concentration determination as described above. Average antibody concentration at each time point was used for calculating the pharmacokinetic parameters using non-compartmental analysis (PK solutions 2.0, Summit Research Services, USA).

Measurement of viral RNA by qRT-PCR

Viral load in lungs of SARS-CoV-2 infected mice (200 PFU) treated with the MD65 antibody, was quantified by qRT-PCR and by plaque assay (see above). Lungs were grinded in 1.5 ml PBS and 200 µl were added to LBF lysis buffer. RNA was extracted using RNAdvance Viral Kit on a Biomek i7 automated workstation (Beckman Coulter, IN), according to the manufacturer's protocol. Each sample was eluted in 50 µl of RNase-free water. RT-PCR was performed using the SensiFASTTM Probe Lo-ROX One-Step kit (Bioline, UK). Primers and probe sequences, targeting the SARS-CoV-2 E gene, were based on the Berlin protocol published in the WHO recommendation for the detection of SARS-CoV-2 [E_Sarbeco_F1 ACAGGTACGTTAATAGT TAATAGCGT, E_Sarbeco_R2 ATATTGCAGCAGTACGCACACA, E_Sarbeco_P1 ACACTAGCCATCCTTACTGCGCTTCG]. The primers and probe were used at a final concentrations of 600 nM and 300 nM, respectively. The thermal cycling reaction was performed at 48°C for 20 min for reverse transcription, followed by 95°C for 2 min, and then 45 cycles of: 15 s at 94°C; 35 s at 60°C for the E gene amplification. Cycle Threshold (Ct) values were converted to PFU equivalents (PFU Eqv.), according to a calibration curve determined in parallel.

Lung histology

Lungs were rapidly isolated, fixed in 4% PBS-buffered paraformaldehyde at room temperature for one week, followed by routine processing for paraffin embedding. Serial sections, 5 µm-thick, were cut and selected sections were stained with hematoxylin and eosin (H&E) and examined by light microscopy. Camera images were taken using a Zeiss Axioskop microscope (Zeiss, Oberkochen, Germany) equipped with a Nikon DS-Ri1 camera controlled by a DS-U3 Digital Sight and the Nis-Elements-Br software suite (Nikon, Tokyo, Japan).

Results and Discussion

Reformatting and characterization of the MD65 antibody. The initial binding and neutralization characterization of MD65 Ab were conducted following the expression of this antibody as a single-chain human-Fc recombinant form (scFv-Fc)[11]. Here, towards implementation of this antibody as a *bona-fide* therapeutic product appropriate for human use, it was re-cloned and produced as a full recombinant IgG molecule of the IgG1/k isotype which includes the triple mutation M252Y/S254T/T256E (YTE) in the Fc region. These modifications increase the antibody affinity towards the human FcRn[33] at acidic pH and thereby prolong its serum half-life, a parameter that is essential for a high therapeutic value[34-36]. Characterization of three versions of the MD65 Ab: scFv-Fc, IgG and IgG-YTE, established that overall they are comparable with regard to their antigen-binding performance (Fig. 1a) and that the IgG versions exhibit slightly favorable affinity when compared to the scFv-Fc one (apparent K_D of 0.7 nM versus 1.0 nM, respectively). Similarly, the two MD65 IgG formats possess equivalent SARS CoV-2 neutralization potency *in vitro* (NT_{50} of 40 ng/ml) which is slightly better than that of the scFv-Fc antibody (NT_{50} of 67 ng/ml; Fig. 1b). In addition, all three Ab versions were shown to effectively prevent the binding of SARS-CoV-2 spike RBD to the hACE2, again with favorable kinetics for the IgG formats (Fig. 1c). These slight differences may indicate that there is a correlation between antibody affinity and SARS CoV-2 neutralization. This aspect will be further clarified in future studies.

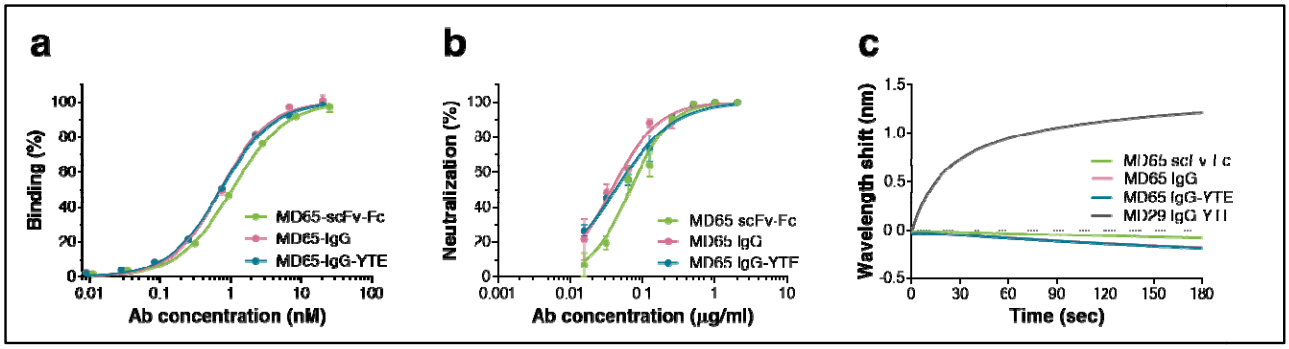

Fig. 1 Characterization of the MD65 Ab versions. a Binding profiles of MD65 Ab variants, tested by ELISA against S1. Values along the curve, depict averages of triplicates ± SEM. **b** SARS-CoV-2 *in vitro* neutralization potency of the MD65 Ab variants evaluated by plaque reduction neutralization test (PRNT). Values are averages of triplicates ± SEM. **c** BLI-determined binding of hACE2 to RBD in the presence of MD65 Ab variants or MD29 IgG-YTE (as a control). Each of the biotinylated antibodies was immobilized on a streptavidin sensor, saturated with RBD, washed and incubated with recombinant hACE2 for 180 sec. Time 0 represents the binding of the hACE2 to the antibody-RBD complex. The MD65 IgG curve completely overlapped with and is therefore masked by the MD65 IgG-YTE.

Pharmacokinetics of MD65 IgG-YTE. A pre-requisite for achieving long circulatory half-life of a given antibody in humans, is to improve its interaction with the FcRn at low pH. We therefore verified that MD65 in its IgG-YTE format, as anticipated, exhibits improved pharmacokinetic abilities compared to the WT IgG format. Accordingly, the interactions of MD65 IgG and IgG-YTE with human FcRn, at pH 6.0 were assessed by biolayer interferometry (BLI). As expected, the modified antibody demonstrated a marked increase in affinity compared to the non-modified version, manifested by a three-fold improved *on*-rate and significant lower *off*-rate of binding (Fig. 2a and b). Steady-state analysis of these interactions revealed that the overall affinity of the IgG-YTE version toward human FcRn at low pH is 10-fold higher than the IgG version (Fig. 2c).

As part of the pre-clinical evaluation of MD65 IgG-YTE antibody and prior to the examination of its therapeutic potency, the pharmacokinetic profiles following intravenous (IV; Fig. 2d) or intraperitoneal (IP; Fig. 2e) administration were determined. Accordingly, MD65 IgG-YTE was first intravenously injected to C57BL/6 mice and plasma antibody levels at various time points were determined by ELISA. The data were fitted by non-compartmental analysis, establishing that MD65 IgG-YTE exhibits a biphasic elimination profile (Fig. 2d), consisting of a typical relatively short distribution phase (α) with a $t_{1/2}$ value of about 180 min and a

significantly longer elimination phase (β) with a $t_{1/2}$ value of about 4,700 min (3.3 days; Fig. 2f). These results are in good agreement with our previous observation that a chimeric protein bearing the same Fc (non YTE) exhibited similar pharmacokinetic parameters in mice[37], corroborating the notion that these mutations do not affect the antibody interaction with the murine FcRn.

The plasma levels of MD65 IgG-YTE following IP administration was then evaluated. The antibody exhibited a rapid and high bioavailability, reaching C_{max} of 40 µg/ml within 180 min (Fig. 2e), a concentration which is commensurate to that measured in the sera at the same time point following IV-administration (49 µg/ml, Fig. 2d). The elimination phase $t_{1/2}$ value following IP administration was approximately 5300 min (3.7 days; Fig. 2f). Therefore, the pharmacokinetic evaluation of the two alternative routes of administration indicate that they both are appropriate for the subsequent protection studies.

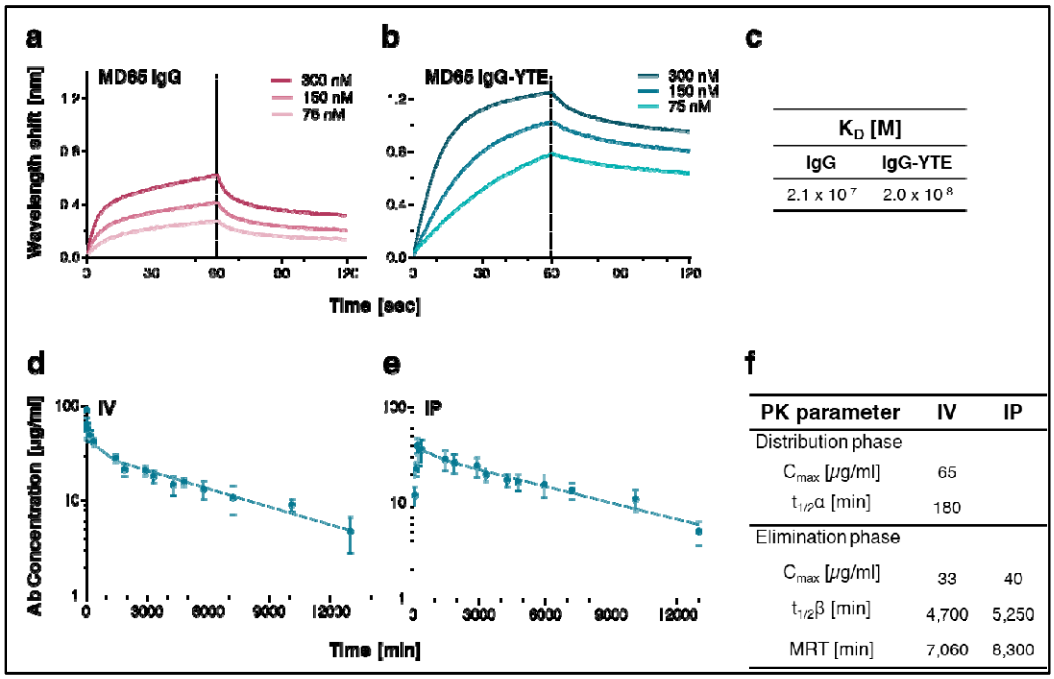

Fig. 2 MD65 binding to human FcRn and pharmacokinetic analysis. a and **b** Kinetics of the interactions between human FcRn and MD65 variants (**a** IgG; **b** IgG-YTE) at pH 6.0, using BLI. Immobilized antibodies were interacted with the indicated concentrations of human FcRn for 60 sec (association phase) followed by a wash step (dissociation phase). **c** Steady-state analysis of sensorgrams by 1:1 binding model was used to determine equilibrium K_D. **d** and **e** Plasma MD65 IgG-YTE concentrations in C57BL/6 mice were determined at the indicated time points following a single (**d**) IV (n=4) or (**e**) IP (n=5) administration of 0.2 mg Ab. Values are expressed as mean ± SEM that were fitted using non-compartmental analysis. **f** Pharmacokinetic parameters of MD65 IgG-YTE.

Protection against SARS-CoV-2 lethal infection in K18-hACE2 transgenic mice. To directly assess the use of the MD65 antibody as the basis for pre- and post-exposure therapy to countermeasure the SARS-CoV-2 infection, the K18-hACE2 transgenic murine model (derived from the C57BL/6 strain), was employed for *in vivo* neutralizing studies. This model was recently shown to fatefully recapitulate the SARS-CoV-2 infection and consequently to serve as a reliable model to predict the efficacy of therapeutic strategies[18,26 27,38].

Infection of K18-hACE2 mice with 200 PFU of the SARS-CoV-2 BavPat1/2020 strain, resulted in significant weight loss from day 5 after infection and death of 80% of the animals by day 9 post infection (Fig. 3). Of note, experiments were conducted both with male and female mice establishing that no sex-dependent significant differences in weight loss or mortality occurred (as exemplified in Supplementary Fig. 1) and in line with previous observations[29].

In order to maintain a steady antibody levels in the circulation for about 8 days (commensurate with the 7.5 days mean time to death (MTTD) in the control group), and taking into consideration the pharmacokinetic profile, the antibody was administered via the IP route in two successive treatments, 4 days apart. In sharp contrast to mock-treated mice (administered with PBS only), pre-exposure IP-administration of the MD65 antibody 4 h before infection (first dose) resulted in full protection of the infected animals without any signs of weight loss (Fig. 3a-c) or any other clinical symptoms. The high lethality of the infection could not be alleviated in mice administered with an isotype antibody control (MH75) that contains the same Fc but targets a non-relevant antigen (ricin)[39].

The successful pre-exposure treatment of the infected mice prompted us to further evaluate the possibility to initiate treatment at even later time-points. K18-hACE2 mice were therefore infected with SARS-CoV-2 and IP-administered (first dose) with the MD65 antibody 1, 2, 3 or 4 days post-infection (dpi). It was found that treatment of infected mice initiated as late as 2 days after infection, was highly efficient in blocking the disease, as demonstrated by the complete prevention of weight loss and, most notably, by total protection of the mice (Fig. 3d-f). Furthermore, even when treatment was initiated 3 dpi, all treated animals survived. Yet, mice in this experimental group displayed some mild symptoms as manifested by a moderate and transient body-weight loss. Even by further delaying the treatment to 4 dpi, a

protection rate of 60% of the infected animals was observed, yet, without a significant delay in the time to death (for the 40% non-surviving animals). The surviving animals in this group regained their initial body weight (Fig. 3e), indicative of efficient recovery.

Taken together, these results demonstrate, for the first time, the therapeutic value of human monoclonal antibodies as a life-saving treatment of severe and lethal COVID-19 infection model.

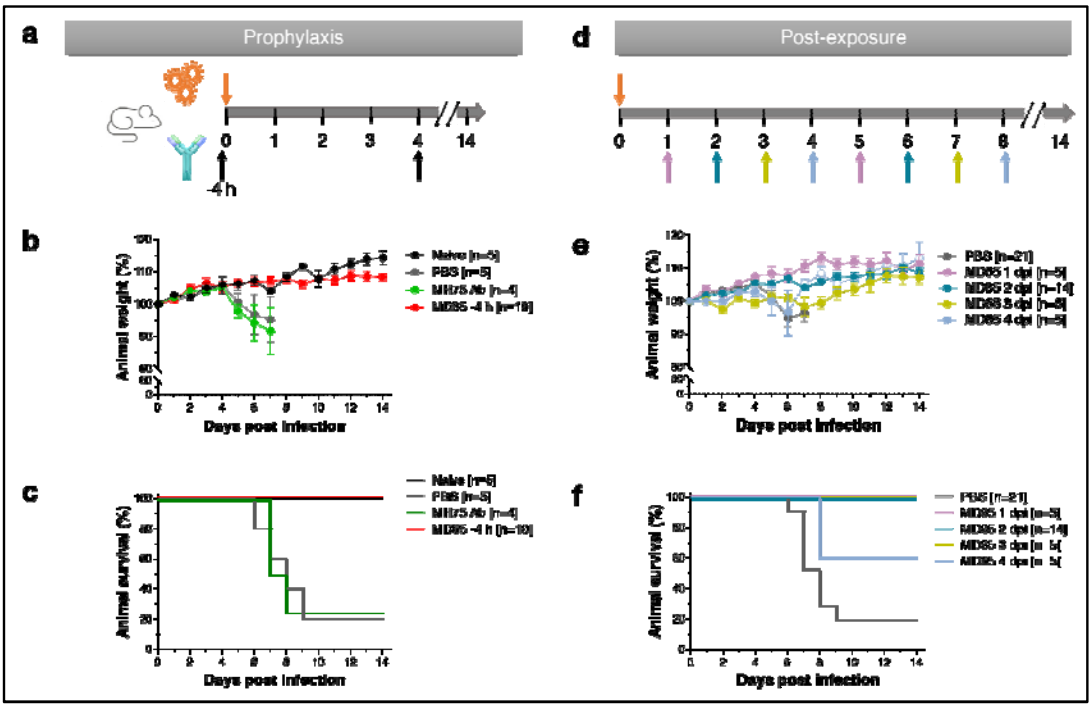

Fig. 3 MD65 Ab-mediated prophylactic and post-exposure protection against SARS-CoV-2 infected K18-hACE2 mice. Prophylactic (**a-c**) or post-exposure (**d-f**) *in vivo* protection experiments**.** Animals were intranasal-infected with 200 PFU of SARS-CoV-2 BavPat1/2020 strain and IP-administered with 1 mg/mouse of MD65 Ab at the indicated time points and 4 days later, for a second time. **a** Schematic description of the experimental design of the prophylactic treatment. **b** Body weight profiles. **c** Kaplan-Meyer surviving curves. Curves describe mice treated with the MD65 antibody (red line), naïve untreated and un-infected animals (black line), animals administered with PBS (grey line) or the isotype control irrelevant-Ab (anti ricin MH75; green line) at the same timepoint as the MD65 treatment. **d** Schematic description of the experimental design of the post-exposure treatment. **e** Body weight profiles. **f** Kaplan-Meyer surviving curves. Curves describe mice treated with the MD65 antibody at various time points post infection, as indicated in the legend within the panel and by the arrows in panel a. Control animals (gray curves) were administered with PBS at day 2 and day 6 after infection. Body weight change is displayed as percentage of initial weight. Only data of the first 7 days is presented in the control groups exhibiting significant mortality. In case of the mice treated 4 dpi (panel e), the weight of the surviving animals is indicated by hollow circles and dashed line. Data represent means ± SEM. The n numbers, indicate the number of animals within each experimental group; when n>5, the

results were combined from several experiments in which each group included at least 4 animals.

SARS-CoV-2 viral load in lungs collected from infected K18-hACE2 mice. The efficiency of the treatment with the MD65 was further established by directly interrogating the viral pulmonary load in infected mice, treated with the antibody 2 dpi (Fig. 4). The lungs were collected 6 dpi (the latest timepoint before onset of mortality) and subjected to qRT-PCR for quantification of the viral burden. The qRT-PCR data indicate that in the control non-treated group, as expected, the SARS CoV-2 virus propagated and reached a very high concentration (Fig. 4a), while antibody treatment resulted in a viral load at least one order of magnitude lower ($p<0.05$).

We further evaluated the infectivity of the virus in the lung by testing its ability to infect VERO E6 cells and to form plaques. As expected, the virus that was isolated from the control group was viable and highly infective (Fig. 4b). However, no infective virus could be isolated from the lungs of the antibody-treated mice (Fig. 4b and Supplementary Fig. 2) establishing that MD65 treatment results in rapid and complete resolution of infection, in agreement with prevention of animal death. This latter finding also suggests that the viral load detected by PCR represents viral debris genomes present in the lungs and not *bona-fide* infective virions.

Lung histopathological evaluation of antibody-treated K18-hACE2 mice. SARS CoV-2 infection of K18-hACE2 mice is manifested by a progressive and widespread viral pneumonia with perivascular and pan-alveolar inflammation, immune cell infiltration, edema, lung consolidation and distinctive vascular system injury that were apparent even three-weeks after infection (in surviving animals)[26,29,40]. Here, the observation that post-exposure antibody-based treatment of infected mice resulted in complete protection with no apparent signs of disease has prompted characterization of the pathological status of their lungs. To this end, mice were infected with SARS CoV-2, treated with MD65 two days later and necropsy was performed at day 21. Overall, no major pathological changes or signs of inflammation were found in the lungs of the antibody-treated mice (Fig. 4c, d and supplementary Fig. 3). The only indication of previous-viral infection is the presence of scarce lymphoid aggregates which are well contained (Fig. 4d). It was previously reported that in the course of SARS CoV-2 infection in the K18-hACE2 model, B-cells infiltrated into the lungs,

accumulated and formed aggregates [29]. It is therefore conceivable to assume that the lymphoid aggregates observed here contain B-cells that were recruited during the initial accumulation of the virus in the lungs, within the first days after infection. Thus, the effective antibody-treatment that inhibited the virus ability to propagate have also prevented the progression of the inflammatory process, as strongly suggested by the infrequent occurrence of pathological changes in the lung and the alveolar tissue. These results substantiate the notion that post-exposure antibody-treatment of lethal SARS CoV-2 infection is highly effective, rapidly neutralizes the virus propagation and limits the inflammatory and the pathological progression.

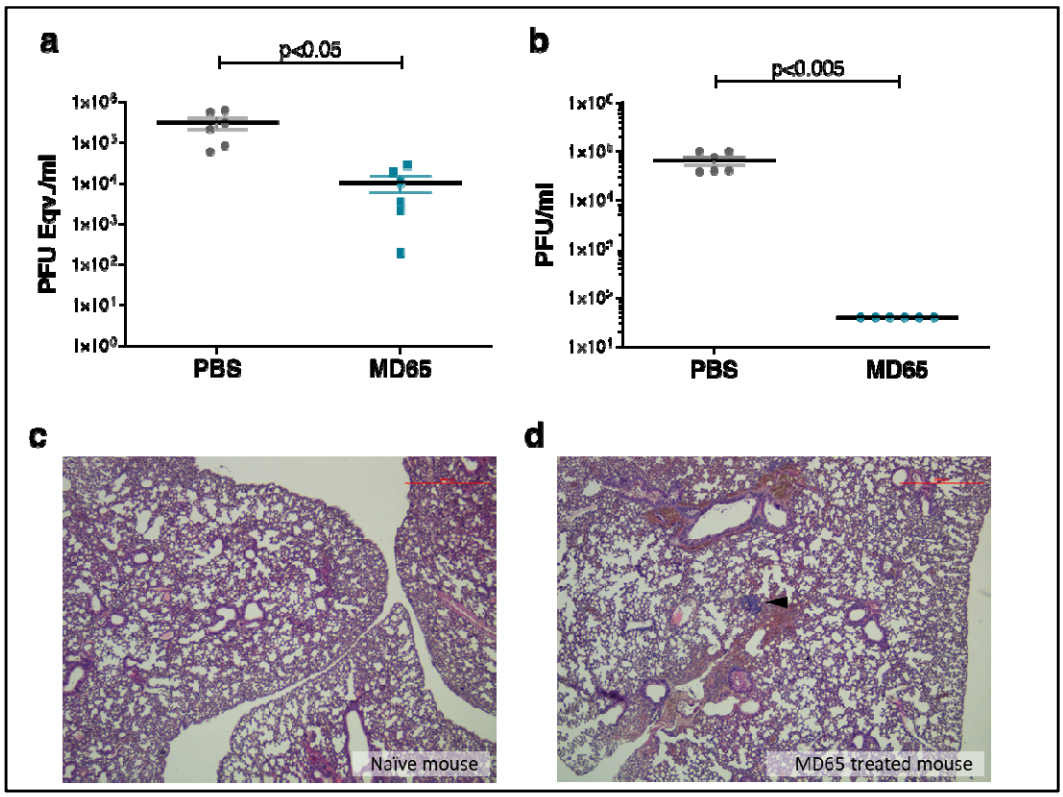

Fig. 4 Viral load determination and histological analysis of lungs, collected from K18-hACE2 mice, infected with SARS-CoV-2 and treated 2 dpi with MD65 antibody. a and **b** Viral load in lung samples, collected 6 dpi from PBS-treated mice (n=6) and mice treated 2 dpi with 1 mg MD65 antibody (n=6). **a** Viral load was quantified by qRT-PCR and expressed as equivalents of PFU/ml. **b** Infectious viral load determined by plaque assay. Dotted line indicates the assay limit of detection. Horizontal bars indicate statistical significance of paired values. **c** and **d** Histological analysis of lung sections, collected 21 dpi from a naïve mouse (**c**) and a mouse that was infected with SARS-CoV-2 and treated 2 dpi with 1 mg MD65 antibody (**d**); Black arrow indicates lymphoid aggregate. The panels include representative images (n=2 for the naïve mice and n=6 for the MD65 treated mice; full images of the lungs are provided in Supplementary Fig. 3). Magnification = 40x.

Anti SARS CoV-2 seroconversion in antibody-treated animals. Antibodies against the SARS-CoV-2 spike protein were reported to be detected as early as 7 days post infection of K18-hACE2 mice[29]. It was previously shown that also following passive immunization (against other infections), surviving animals seroconverted by developing antigen-specific antibodies, which contributed to protection against re-infection[41]. Furthermore, in the context of the current pandemic, since the re-infection by SARS-CoV-2 is a tangible possibility, it was of interest to determine whether the MD65-treated mice developed an endogenous immune response toward the virus.

To this objective, the mouse humoral immune response towards SARS-CoV-2 Spike glycoprotein was measured in treated mice at 14 dpi (Fig. 5). Interestingly, the prophylactic administration of the MD65 Ab prevented the mounting of the humoral response, suggesting that effective neutralization of the virus occurred immediately upon infection (Fig. 5a). In contrast, animals treated either 1- or 2-days post-infection developed a marked antibody response that is in good correlation with the time of treatment. As several studies have shown that most SARS-CoV-2 neutralizing antibodies target the S1 subunit and even more specifically the RBD, the humoral responses of the antibody-treated mice toward these two antigens was further evaluated. Indeed, a similar pattern was observed for these two antigens as for the spike (Fig. 5b and 5c), suggesting that the endogenous antibody response may contain SARS-CoV-2 neutralizing antibodies that will confer partial or full protection against re-infection. Determination of the neutralization titer of these samples could provide further support for this concept, yet such an experiment is complicated by the masking effect of residual MD65 Ab.

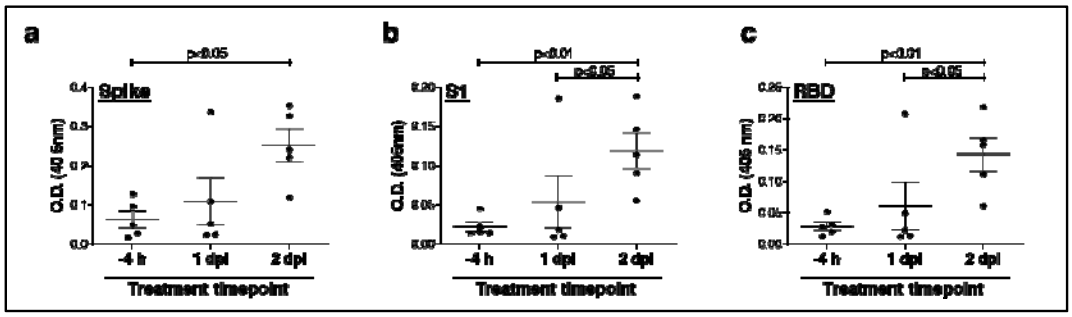

Fig. 5 Endogenous anti-SARS-CoV-2 humoral response of infected K18-hACE2 mice treated with the MD65 antibody. Sera samples were collected at day 14 post-infection from mice treated with MD65 at the indicated timepoints and tested by ELISA for the presence of endogenous (murine) antibodies against the SARS-CoV-2 antigens: (**a**) spike, (**b**) S1 or (**c**) RBD. Data represent individual and mean ±SEM (n=5 mice) of measurements obtained for sera samples at 1:60 dilution. Horizontal bars indicate statistical significance of paired values.

Dose-dependent therapeutic efficacy of MD65. The ability of MD65 to protect K18-hACE2 mice from SARS-CoV-2 infection at lower single doses was further evaluated. To this end, single treatments of either 1, 0.1 and 0.01 mg Ab/animal were administered at day 2 post virus infection. Body weight loss or mortality were not detected in any of the animals treated with doses of 1 or 0.1 mg MD65 (Fig. 6). Conversely, no significant protection was attained by treating animals with the low 0.01 mg MD65 dose. In the latter case, 80% of the mice, exhibited massive weight lost and succumbed to the infection. Yet, it should be noted that this dose of antibody induced a marked delay in the time to death (range 12-14 days with MTTD of 12.5 days) when compared to the control mice (range 7-10 days with MTTD of 8 days).

In conclusion, the dose-dependency experiments established that administration of MD65 as late as 2 dpi, at a dose as low as 0.1 mg/mouse (representing 5 mg/kg body weight) is therapeutically efficient. Furthermore, a therapeutically-relevant delay in MTTD is promoted even at a 10-times lower dose.

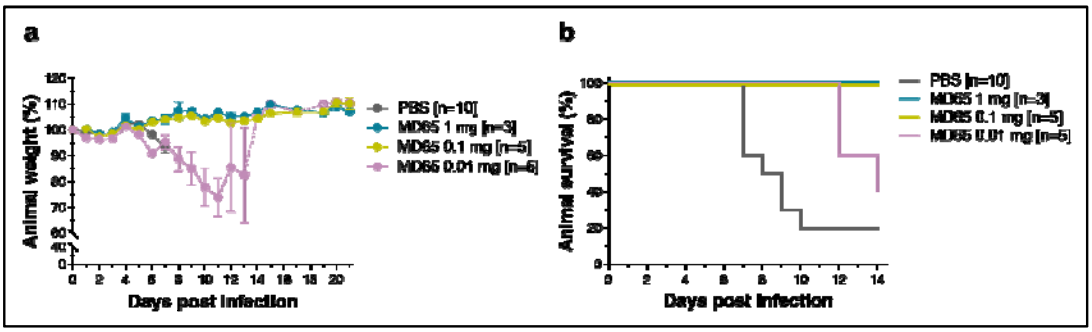

Fig. 6 Dose-dependent therapeutic efficacy of MD65. Single doses of 1, 0.1 and 0.01 mg MD65 Ab/animal were administered at day 2 post viral infection. **a** Body weight profiles. **b** Kaplan-Meyer surviving curves. Curves describe mice treated with the indicated doses of MD65 (see color legend within panels) and control animals, administered with PBS (grey line). Data represent means ± SEM. Body weight change is displayed as percentage of initial weight. Only data of the first 7 days is presented in the control group exhibiting significant mortality. In case of the mice treated with 0.01 mg MD65, the weight of the surviving animal is indicated by hollow circles and dashed line.

Antibody dependent enhancement (ADE) of infection was documented for several viruses including respiratory syncytial virus (RSV), measles as well as for corona viruses[42]. This phenomenon is usually associated with the enhancement of virus uptake by phagocytic cells or by the formation of immune complexes that lead to

excessive inflammatory responses. Post-exposure treatment of infected animals, where the possibility for the formation of immune-complexes is higher, was proposed as one of the tests for possible ADE effects in general and of SARS CoV-2 in particular[42]. As of today, ADE was not reported for the current pandemic, yet there is a need to continue monitoring for such effect[43]. In the current study, no worsened effect (in terms of mortality, body weight loss as well as increased viral burden in the lungs) in the antibody treated animals was observed, in spite of the high sensitivity of the K18-hACE2 model which could have detected with ease such an occurrence.

To conclude, the data presented in this report demonstrates for the first time, to the best of our knowledge, high-effective post-exposure therapy of SARS-CoV-2 lethal infection in an animal model using a fully human monoclonal antibody. From the clinical point of view, the efficacy of this antibody extends the therapeutic window permitting initiation of life-saving treatment at late stages post-infection. This study incents the development of a clinical product based on the MD65 antibody for human use.

Acknowledgments

We thank Prof. Dr. Christian Drosten at the Charité Universitätsmedizin, Institute of Virology, Berlin, Germany for providing the SARS-CoV-2 BavPat1/2020 strain. We wish to express our gratitude to our colleagues Dr. Hagit Achdout, Dr. Nir Paran, Dr. Emanuelle Mamroud, Dr. Hadas Tamir, Dr. Yfat Yahalom-Ronen, Dr. Shay Weiss, Dr. Hadar Marcus, Dr. Noa Madar-Balakirski, Roy Avraham, Dr. Amir Ben-Shmuel, Dr. Amir Rosner, Dr. Tseela David and Dr. Hani Dekel Jaoui for fruitful discussions and support. We would like to thank Moshe Mantzur, Tamar Aminov, Meni Girshengorn and Sarah Borni for skillful and devoting technical assistance.

Author Contributions

R.R., T.N-P., A.M., E.M., Y.L., R.A., R.F., M.A., E.E., D.G., E.B.V., S.M., B.P., A.Z., S.L., A. B-D, Y.E. and O.M. designed, carried out and analyzed the data. T.C., S.Y., S.S and T.I. added fruitful discussions, reviewed and edited the manuscript. R.R. and O.M. supervised the project. All authors have approved the final manuscript.

Competing Interests

Patent application for the described antibody was filed by the Israel Institute for Biological Research. None of the authors declared any additional competing interests.

Data and materials availability

All data are available from the corresponding authors upon reasonable request. Antibody is available (by contacting Ohad Mazor from the Israel Institute for Biological Research; ohadm@iibr.gov.il) for research purposes only under an MTA, which allows the use of the antibody for non-commercial purposes but not its disclosure to third parties.

References

1 Corti, D. *et al.* Prophylactic and postexposure efficacy of a potent human monoclonal antibody against MERS coronavirus. *Proc Natl Acad Sci U S A* **112**, 10473-10478, doi:10.1073/pnas.1510199112 (2015).

2 Rockx, B. *et al.* Structural basis for potent cross-neutralizing human monoclonal antibody protection against lethal human and zoonotic severe acute respiratory syndrome coronavirus challenge. *J Virol* **82**, 3220-3235, doi:10.1128/JVI.02377-07 (2008).

3 Zhu, Z. *et al.* Potent cross-reactive neutralization of SARS coronavirus isolates by human monoclonal antibodies. *Proc Natl Acad Sci U S A* **104**, 12123-12128, doi:10.1073/pnas.0701000104 (2007).

4 Chen, Z. *et al.* Human Neutralizing Monoclonal Antibody Inhibition of Middle East Respiratory Syndrome Coronavirus Replication in the Common Marmoset. *J Infect Dis* **215**, 1807-1815, doi:10.1093/infdis/jix209 (2017).

5 Scheid, J. F. *et al.* Broad diversity of neutralizing antibodies isolated from memory B cells in HIV-infected individuals. *Nature* **458**, 636-640, doi:10.1038/nature07930 (2009).

6 Cohen, J. Antibodies may curb pandemic before vaccines. *Science* **369**, 752-753, doi:10.1126/science.369.6505.752 (2020).

7 Ju, B. *et al.* Human neutralizing antibodies elicited by SARS-CoV-2 infection. *Nature* **584**, 115-119, doi:10.1038/s41586-020-2380-z (2020).

8 Liu, L. *et al.* Potent neutralizing antibodies against multiple epitopes on SARS-CoV-2 spike. *Nature* **584**, 450-456, doi:10.1038/s41586-020-2571-7 (2020).

9 Yuan, M. *et al.* Structural basis of a shared antibody response to SARS-CoV-2. *Science* **369**, 1119-1123, doi:10.1126/science.abd2321 (2020).

10 Zost, S. J. *et al.* Potently neutralizing and protective human antibodies against SARS-CoV-2. *Nature* **584**, 443-449, doi:10.1038/s41586-020-2548-6 (2020).

11 Noy-Porat, T. *et al.* A panel of human neutralizing mAbs targeting SARS-CoV-2 spike at multiple epitopes. *Nat Commun* **11**, 4303, doi:10.1038/s41467-020-18159-4 (2020).

12 Baum A *et al.* REGN-COV2 antibodies prevent and treat SARS-CoV-2 infection in rhesus macaques and hamsters. *science* **Oct 9**, doi: 10.1126/.abe2402. (2020).

13 Mor M *et al.* Multi-Clonal Live SARS-CoV-2 In Vitro Neutralization by Antibodies Isolated from Severe COVID-19 Convalescent Donors. *BioRxiv*, doi: https://doi.org/10.1101/2020.10.06.323634 (2020).

14 Tortorici, M. A. *et al.* Ultrapotent human antibodies protect against SARS-CoV-2 challenge via multiple mechanisms. *Science*, doi:10.1126/science.abe3354 (2020).

15 Johansen, M. D. *et al.* Animal and translational models of SARS-CoV-2 infection and COVID-19. *Mucosal Immunol*, doi:10.1038/s41385-020-00340-z (2020).

16 Bao, L. *et al.* The pathogenicity of SARS-CoV-2 in hACE2 transgenic mice. *Nature* **583**, 830-833, doi:10.1038/s41586-020-2312-y (2020).

17 Dinnon, K. H., 3rd *et al.* A mouse-adapted model of SARS-CoV-2 to test COVID-19 countermeasures. *Nature*, doi:10.1038/s41586-020-2708-8 (2020).

18 Golden, J. W. *et al.* Human angiotensin-converting enzyme 2 transgenic mice infected with SARS-CoV-2 develop severe and fatal respiratory disease. *JCI Insight*, doi:10.1172/jci.insight.142032 (2020).

19 Hassan, A. O. *et al.* A SARS-CoV-2 Infection Model in Mice Demonstrates Protection by Neutralizing Antibodies. *Cell* **182**, 744-753 e744, doi:10.1016/j.cell.2020.06.011 (2020).

20 Jiang, R. D. *et al.* Pathogenesis of SARS-CoV-2 in Transgenic Mice Expressing Human Angiotensin-Converting Enzyme 2. *Cell* **182**, 50-58 e58, doi:10.1016/j.cell.2020.05.027 (2020).

21 Letko, M., Marzi, A. & Munster, V. Functional assessment of cell entry and receptor usage for SARS-CoV-2 and other lineage B betacoronaviruses. *Nat Microbiol* **5**, 562-569, doi:10.1038/s41564-020-0688-y (2020).
22 Lutz, C., Maher, L., Lee, C. & Kang, W. COVID-19 preclinical models: human angiotensin-converting enzyme 2 transgenic mice. *Hum Genomics* **14**, 20, doi:10.1186/s40246-020-00272-6 (2020).
23 Moreau, G. B. *et al.* Evaluation of K18-hACE2 Mice as a Model of SARS-CoV-2 Infection. *Am J Trop Med Hyg* **103**, 1215-1219, doi:10.4269/ajtmh.20-0762 (2020).
24 Sun, J. *et al.* Generation of a Broadly Useful Model for COVID-19 Pathogenesis, Vaccination, and Treatment. *Cell* **182**, 734-743 e735, doi:10.1016/j.cell.2020.06.010 (2020).
25 Wan, Y., Shang, J., Graham, R., Baric, R. S. & Li, F. Receptor Recognition by the Novel Coronavirus from Wuhan: an Analysis Based on Decade-Long Structural Studies of SARS Coronavirus. *J Virol* **94**, doi:10.1128/JVI.00127-20 (2020).
26 Winkler, E. S. *et al.* SARS-CoV-2 infection of human ACE2-transgenic mice causes severe lung inflammation and impaired function. *Nat Immunol*, doi:10.1038/s41590-020-0778-2 (2020).
27 Zheng, J. *et al.* K18-hACE2 Mice for Studies of COVID-19 Treatments and Pathogenesis Including Anosmia. *bioRxiv*, doi:10.1101/2020.08.07.242073 (2020).
28 Sun, S. H. *et al.* A Mouse Model of SARS-CoV-2 Infection and Pathogenesis. *Cell Host Microbe* **28**, 124-133 e124, doi:10.1016/j.chom.2020.05.020 (2020).
29 Yinda, C. K. *et al.* K18-hACE2 mice develop respiratory disease resembling severe COVID-19. *bioRxiv*, doi:10.1101/2020.08.11.246314 (2020).
30 Alsoussi, W. B. *et al.* A Potently Neutralizing Antibody Protects Mice against SARS-CoV-2 Infection. *J Immunol* **205**, 915-922, doi:10.4049/jimmunol.2000583 (2020).
31 Case, J. B. *et al.* Neutralizing Antibody and Soluble ACE2 Inhibition of a Replication-Competent VSV-SARS-CoV-2 and a Clinical Isolate of SARS-CoV-2. *Cell Host Microbe*, doi:10.1016/j.chom.2020.06.021 (2020).
32 Rogers, T. F. *et al.* Isolation of potent SARS-CoV-2 neutralizing antibodies and protection from disease in a small animal model. *Science* **369**, 956-963, doi:10.1126/science.abc7520 (2020).
33 Dall'Acqua, W. F., Cook, K. E., Damschroder, M. M., Woods, R. M. & Wu, H. Modulation of the effector functions of a human IgG1 through engineering of its hinge region. *J Immunol* **177**, 1129-1138, doi:10.4049/jimmunol.177.2.1129 (2006).
34 Gaudinski, M. R. *et al.* Safety and pharmacokinetics of the Fc-modified HIV-1 human monoclonal antibody VRC01LS: A Phase 1 open-label clinical trial in healthy adults. *PLoS Med* **15**, e1002493, doi:10.1371/journal.pmed.1002493 (2018).
35 Oganesyan, V. *et al.* Structural insights into neonatal Fc receptor-based recycling mechanism. *The Journal of Biological Chemistry* **289**, 7812-7824 (2014).
36 Yu, X. Q. *et al.* Safety, Tolerability, and Pharmacokinetics of MEDI4893, an Investigational, Extended-Half-Life, Anti-Staphylococcus aureus Alpha-Toxin Human Monoclonal Antibody, in Healthy Adults. *Antimicrob Agents Chemother* **61**, doi:10.1128/AAC.01020-16 (2017).
37 Noy-Porat, T. *et al.* Acetylcholinesterase-Fc Fusion Protein (AChE-Fc): A Novel Potential Organophosphate Bioscavenger with Extended Plasma Half-Life. *Bioconjug Chem* **26**, 1753-1758, doi:10.1021/acs.bioconjchem.5b00305 (2015).
38 Jia, H., Yue, X. & Lazartigues, E. ACE2 mouse models: a toolbox for cardiovascular and pulmonary research. *Nat Commun* **11**, doi:https://doi.org/10.1038/s41467-020-18880-0 (2020).
39 Noy-Porat, T. *et al.* Extended therapeutic window for post-exposure treatment of ricin intoxication conferred by the use of high-affinity antibodies. *Toxicon* **127**, 100-105, doi:10.1016/j.toxicon.2017.01.009 (2017).
40 Oladunni, F. S. *et al.* Lethality of SARS-CoV-2 infection in K18 human angiotensin-converting enzyme 2 transgenic mice. *Nat Commun* **11**, 6122, doi:10.1038/s41467-020-19891-7 (2020).

41 Rosenfeld, R. *et al.* Isolation and chimerization of a highly neutralizing antibody conferring passive protection against lethal Bacillus anthracis infection. *PLoS One* **4**, e6351, doi:10.1371/journal.pone.0006351 (2009).

42 Lee, W. S., Wheatley, A. K., Kent, S. J. & DeKosky, B. J. Antibody-dependent enhancement and SARS-CoV-2 vaccines and therapies. *Nat Microbiol* **5**, 1185-1191, doi:10.1038/s41564-020-00789-5 (2020).

43 Arvin, A. M. *et al.* A perspective on potential antibody-dependent enhancement of SARS-CoV-2. *Nature* **584**, 353-363, doi:10.1038/s41586-020-2538-8 (2020).

44 Yahalom-Ronen, Y. *et al.* A single dose of recombinant VSV-ΔG-spike vaccine provides protection against SARS-CoV-2 challenge *bioRxiv*, doi:10.1101/2020.06.18.160655 (2020).

45 Finkel, Y. *et al.* The coding capacity of SARS-CoV-2. *Nature*, doi:10.1038/s41586-020-2739-1 (2020).